The dripping of a crystal

R. Ishiguro, F. Graner*, E. Rolley, and S. Balibar
Laboratoire de Physique Statistique de l'Ecole Normale Supérieure
associé aux Universités Paris 6 et Paris 7 et au CNRS
24 rue Lhomond 75231 Paris Cedex 05, France

and J. Eggers
School of Mathematics, University of Bristol, University Walk, Bristol BS8 1TW, United Kingdom

Dripping is usually associated with fluid motion, but here we describe the analogous phenomenon of a ^{3}He crystal growing and melting under the influence of surface tension and gravity. The pinch-off of the crystal is described by a purely geometric equation of motion, viscous dissipation or inertia being negligible. In analogy to fluid pinch-off, the minimum neck radius R_n goes to zero like a power law, but with a new scaling exponent of 1/2. However, for most of the neck's evolution the scaling exponent is found to be much closer to 1/3. We attribute this behavior to slowly decaying transients of the pinch solution, making the "critical region" very small, both in time and space. We argue that there is no universal law governing the recoil of crystal tips after pinch-off, but for very early times our experiments are consistent with an approximate theory predicting an asymptotic regime with exponent 1/2.

PACS numbers: 47.15.-x, 67.80.-s, 68.35.Ja, 68.08.-p

I. INTRODUCTION

A liquid jet coming out of a nozzle is unstable: due to capillary forces, it splits into droplets: this is the well known Plateau instability [1]. When the drop detaches at a critical time t_s, its neck radius R_n tends to zero and the equations of hydrodynamics form a singularity. The profiles near the singularity are self-similar, and R_n goes to zero linearly in time [2]. In the case that viscosity is negligible and the dynamics is dominated by inertial effects, a different critical behavior was found, and the exponent becomes 2/3 [3, 4].

Here we present a third situation where both viscous dissipation in the bulk and inertial effects are negligible. This is the unusual case of crystals whose shape evolves by local growth and melting in a situation where the temperature is very homogeneous so that the driving forces are gravity and surface tension, as for usual liquids. Dripping becomes a purely geometrical effect for which simple arguments lead to the prediction $R_n \propto \Delta t^{1/2}$, where $\Delta t = |t - t_s|$. We were surprised to find a $\Delta t^{1/3}$ behavior in the experiment but, as we shall see, our results are compatible with a 1/2 exponent for very small radii, and numerical simulations confirm that this asymptotic behavior is reached at very small R_n only.

Helium crystals are known to change shape rather quickly by local crystallization and melting [5]. These crystals are very pure and can be studied in equilibrium or close to equilibrium with liquid helium in cells where the temperature is very homogeneous. As a result, their shape is governed by gravity and surface tension, not by temperature nor by concentration gradients as usual crystals. Except when facets come into play, the evolution of their shape looks like that of flowing liquids; there is no mass transport inside the crystals themselves, only some in the surrounding liquid which allows local crystallization and melting. The dynamics of ^{4}He crystals is very fast at low temperature [5]. The dynamics of ^{3}He crystals is not as fast as that of ^{4}He but still much faster than classical crystals: their shape relaxes typically in a few seconds at 0.32 K, the temperature of the minimum in the melting curve where the latent heat is zero. At that temperature, ^{3}He crystals are not facetted and they look like transparent drops of some viscous fluid like honey although they are high quality crystals. We have recorded

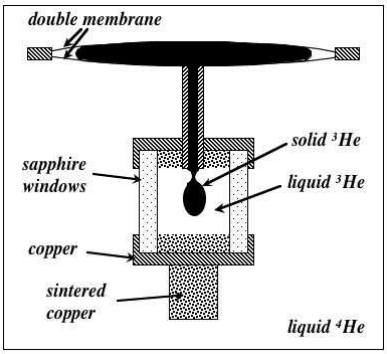

FIG. 1: The experimental cell where ^{3}He crystals were grown thanks to a flexible membrane. The lower part was 3.45 mm wide and 3.27 mm high; it could be observed through windows from the outside of the cryostat, as shown in Fig. 2.

*Present address: Laboratoire de Spectrométrie Physique, associé au CNRS et à l'Université J. Fourier - Grenoble I, BP 87, 38402 Saint Martin d'Hères Cedex, France

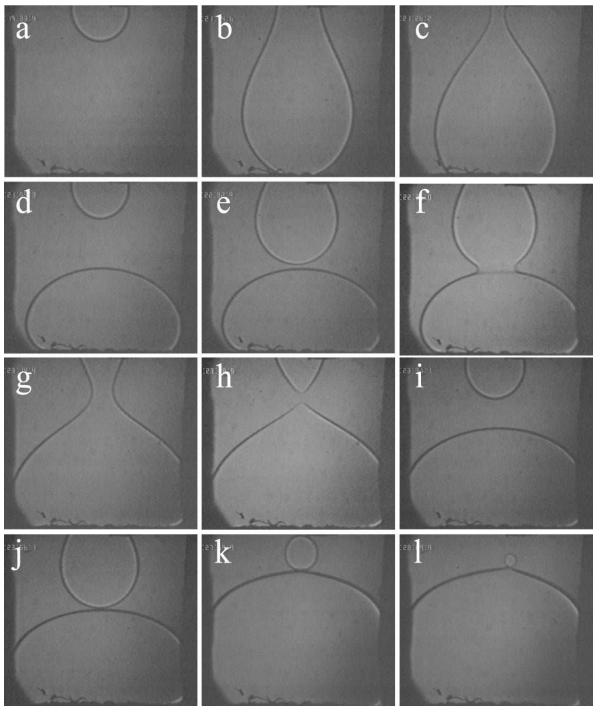

FIG. 2: Twelve images (of width 3.5 mm) showing how a ^{3}He crystal "flows" down from the upper part of the cell into its lower part. For this recording, which took a few minutes, the temperature was T_{min} + 11 mK. The crystal first "drips" down, so that a crystalline "drop" forms at the bottom (a to c); then a second drop appears (d) and comes into contact with the first one (e); coalescence is observed (f) and was quantitatively analyzed in [6]. It is followed by the dripping of a second drop which has exactly the same crystalline orientation as the first one because this is not real flow, it is local melting and growth of a single crystal which keeps the same orientation all the time. it drips down and coalescence occurs again (j). Usually, the last drop (k) behaves differently because, being smaller than the orifice, it falls in the liquid and changes orientation before touching the lower crystal. As a consequence, there is a grain boundary between the two crystals which do not coalesce; the last drop keeps round, moves to the right and finally vanishes (l). At this temperature, ^{3}He crystals have no facets, they are rough in all directions.

the time evolution of their shape with an ordinary CCD camera.

In a previous article [6], we have taken advantage of the properties of these ^{3}He crystals to investigate the coalescence of crystalline drops. By analyzing video sequences which had been recorded earlier by some of us [7] we could verify a prediction by Maris [8] for the time evolution of the neck which forms when two crystalline drops come into contact. We found good agreement with theory, and it confirmed that, with such crystals, coalescence is a purely geometrical problem: as we shall see, the local velocity dR_n/dt, which is the time derivative of the neck radius is simply related to the local curvature $1/R_n$.

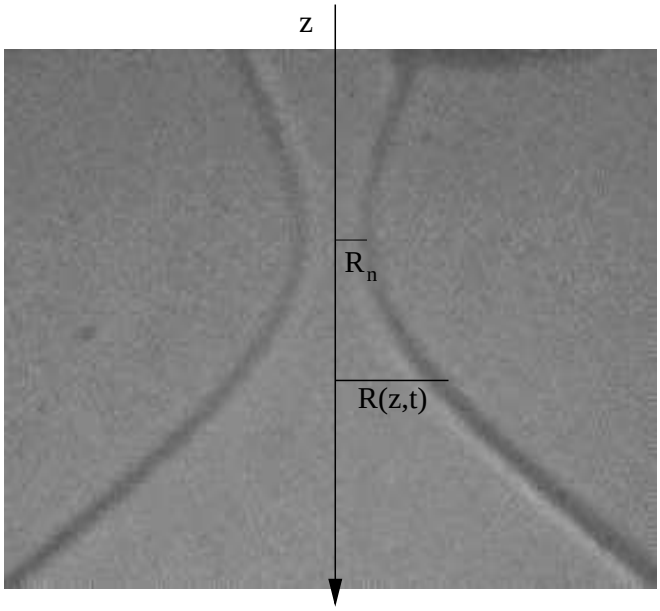

FIG. 3: Just before separation of the two crystalline drops, the neck shape is symmetric, contrary to what is usually observed with liquids.

II. THEORY

The driving force for growth is the difference $\Delta\mu$ between the chemical potential μ_L (per unit mass) of the surrounding liquid and that of the crystal, μ_C. It is linearly related to the growth velocity of the crystal v_n by the relation [9] (p.74)

$$v_n = k\,\Delta\mu. \tag{1}$$

The mobility k has been calculated and measured experimentally [5]. Near $T_{\rm min} = 0.32$ K, it is given by

$$k^{-1} = 5.5 + (3.9 \times 10^4)(T - T_{\rm min})^2 \text{ m/s} \tag{2}$$

with T in K [7].

Assuming that the crystal grows at constant strain, $\Delta\mu$ can be calculated from a mechanical equilibrium between the liquid and solid [9], p.18. Neglecting the anisotropy of the surface tension γ, which is small for bcc crystals such as ^{3}He, this gives $\Delta\mu\rho_C = \delta p_L \Delta\rho/\rho_L - \gamma\kappa$, where κ is the local curvature and δp_L is the pressure in the liquid relative to some reference value. The physical constants are $\gamma = 0.06$ erg/cm^2 [10] (surface tension) and $\Delta\rho = \rho_C - \rho_L = 5.7 \times 10^{-3}$ g/cm^3 (density difference). The liquid pressure δp_L includes a hydrostatic contribution; we will approximate δp_L by a constant, since the capillary length $\ell_c = \sqrt{\gamma/(\Delta\rho g)} = 1.026$ mm is large compared to the size of the pinch region.

If the radius of the axisymmetric crystal is $R(z,t)$ (cf. Fig. 3), the shape of the crystal changes according to

$$\dot{R} = \sqrt{1 + R'^2}\, k \Delta\mu, \tag{3}$$

where dot and prime are the derivatives with respect to the time and space, respectively. We nondimensionalize R with respect to the radius of the nozzle $R_0 = 0.5$ mm: $h(x,\tau) = R(z,\Delta t)/R_0$, where $x = z/R_0$ and time is rescaled according to $\tau = \Delta t k\gamma/(R_0^2\rho_C)$. Then (3) leads to

$$\frac{dh}{d\tau} = -\frac{1}{h} + \frac{h''}{1+h'^2} + \Delta\sqrt{1+h'^2}, \qquad (4)$$

where Δ is the non-dimensionalized departure of the liquid pressure from the value corresponding to equilibrium. The first two terms on the right come from the mean curvature of the crystal surface.

To initiate pinch-off, we will set Δ to a small negative value in the simulations to be reported below. The radial curvature (first term on the left), drives pinch-off as expected: a melting of the crystal (reduction in h and thus in surface area) leads to a lower energy state. For small h, equation (4) is dominated by the mean curvature terms, and thus reduces to the famous (axisymmetric) mean curvature flow, which has been studied extensively in the Mathematics literature [11, 12]. In particular, this equation exhibits blow-up at a finite time $\tau = 0$, corresponding to the pinch-off seen in Fig.2. If the second (axial) curvature term is negligible near the minimum $h_{min} = R_n/R_0$ of the profile, one ends up with the simple equation $\dot{h}_{min}h_{min} = -1$. This can be integrated to give

$$h_{min}^2 = 2\tau, \qquad (5)$$

which is indeed the correct asymptotics for the pinching of the neck, as we are going to see below. However, contributions from the axial curvature are only *logarithmically* subdominant, so the convergence toward (5) is exceedingly slow.

Before comparing the above prediction with experiment, we need to describe more precisely how this experiment was done. As already explained in refs. 6 and 7, ^{3}He crystals were grown at 0.32 K in a cell which had two parts connected by a vertical capillary (see Fig. 1) and it was immersed in a ^{4}He liquid bath which provided a good thermal homogeneity. When increasing the pressure of liquid ^{4}He, the double membrane in the upper part of the ^{3}He cell was deformed and the ^{3}He pressure increased. When the ^{3}He crystallization pressure was reached, the first crystal seed happened to nucleate in the upper part. It was grown by increasing the ^{4}He pressure further. When the ^{3}He crystal was large enough, it started invading the lower part, and became visible at the lower end of the capillary (see Fig. 2a). At that moment, the pressure was fixed and the shape evolved at constant *total* crystal volume. By exchanging mass with its liquid phase, i.e. by local growth and melting, the ^{3}He crystal started to move down because of gravity.

At $T_{min} = 0.32$ K, the latent heat vanishes and the liquid-solid transition is sensitive to T only to second order in $(T - T_{min})$. At the surface of ^{3}He crystals, facets

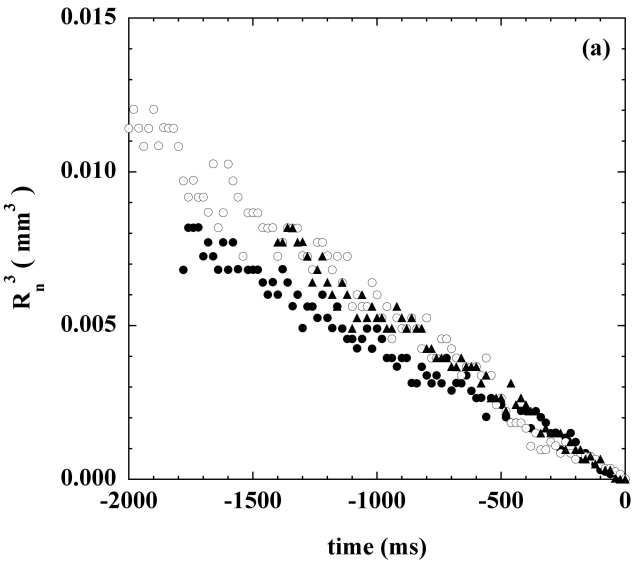

FIG. 4: The cube of the neck radius R_n is linearly related to the time Δt before the singularity, where the two crystals separate from each other. Different symbols correspond to different recordings at T_{min} + 9 mK.

appear only below 100 mK [5, 13–15], and the dynamics of the liquid-solid interface is governed by (1) and (2). Since the measurements were done at $T_{min} + 9$ mK where the growth resistance is $k^{-1} = 0.115$ s/m, (5) predicts the asymptotic behavior $R_n^2 = (1.145 \times 10^{-4})\Delta t$ mm^2 with Δt in ms, a prediction that contains no adjustable parameters.

As shown in Fig. 2, the transfer of the ^{3}He crystal from the upper part of the cell to the lower visible part occurs by successive dripping (b,c and g,h) and coalescence events (e,f and j). Here, we analyze the dripping. Fig. 3 shows that the shape of the neck is symmetric with respect to a horizontal plane, contrary to what is observed for ordinary fluids. We have analyzed the time variation of the neck radius R_n and attempted to find the scaling exponent with which the minimum neck radius vanishes by plotting appropriate powers of R_n as function of time. Figure 4 shows that by plotting R_n^3 one finds the closest approximation of a straight line over the entire time period. This observation seems to contradict (5), which predicts an exponent of 1/2 as opposed to 1/3 supported by experiment. We will see below that the explanation for this apparent discrepancy is that the asymptotic behavior (5) is only observed for times extremely close to the singularity.

To understand the nature of the convergence toward the asymptotic solution, it is crucial to look at a more complete description, which includes the spatial structure of the solution. We begin by rewriting the solution in a different coordinate system:

$$h(x,\tau) = \tau^{1/2}\phi(\xi, l_\tau), \quad \xi = (x - x_0)/\tau^{1/2}, \qquad (6)$$

where $l_\tau = |\ln(\tau)|$ and x_0 is the point where pinch-off occurs. For fluids, the solution converges very quickly to a similarity function ϕ which is in fact *independent* of l_τ [2, 16]. This means that profiles, taken at different times, are related to each other simply by a rescaling of the coordinate axes. In many cases involving the breakup of liquid threads or jets, measurements of the minimum radius or of the entire profile show excellent agreement with similarity theory [1, 17–19].

However, the similarity structure of the pinch-off solution of (4) is different in two important respects [12], the similarity function being

$$\phi(\xi, l_\tau) = \sqrt{2}\left(1 + \frac{\xi^2 - 2}{4l_\tau} + O\left(\frac{\ln(l_\tau)}{l_\tau^2}\right)\right). \qquad (7)$$

Note that (7) is symmetric in space, in agreement with observation (cf. Fig. 3). Firstly, ϕ contains a contribution which depends explicitely on the logarithmic time l_τ; this contribution comes from the axial curvature of the interface. In the asymptotic limit $l_\tau \to \infty$ (5) is recovered for $\xi = 0$, but only on a logarithmic scale, as opposed to the rapid convergence of classical similarity solutions. Secondly, the convergence to the similarity form is not uniform [16], but only in a small region around the neck which is of the same size as the minimum neck radius itself, such that the similarity variable ξ remains of order one. This can be seen from the next order in an expansion in $1/l_\tau$, which we performed recently [20]. Namely, for the higher order terms to be small, $|\xi|$ must be small compared to $\sqrt{l_\tau}$. For all practical purposes, the latter is never much larger than unity. Note also the appearance of *logarithms* of $\ln(\tau)$ appearing at second order in (7), implying a very slow convergence indeed.

Singularities in which the logarithm l_τ appears explicitly are called "type II singularities" [21]. Mathematically, they come about as follows: if the equations of motion are rewritten in the coordinate system described by (6), the singularity appears as a *fixed point*. For the singularity to be observed, the dynamics must be driven toward the fixed point, which means that all eigenvalues of the linearization must be negative: this is known as "type I singularity". Mean curvature flow belongs to the "critical" case in which one of the eigenvalues is zero. A careful analysis reveals that the singularity is reached, but only on a logarithmic scale, cf. (7). However, this effect has never been estimated quantitatively. Our recent results show that the second order contribution to (7) is still universal [20], as confirmed by the numerical simulations reported below. We suspect this remains true at higher orders, but this still needs to be investigated.

III. NUMERICS AND COMPARISON TO EXPERIMENT

In order to understand the approach to the asymptotic behavior (5) we performed numerical simulations of the axisymmetric mean curvature flow equation (4), including gravity. We used an implicit, second order, finite difference method as developed originally for the fluid drop pinch-off problem in [22]. As h_{min} decreases, smaller features need to be resolved near the neck. We use an automatic mesh refinement as developed in [23] to make sure all parts of the solution are well resolved. This permits to follow the solution through 7 orders of magnitude in the neck radius.

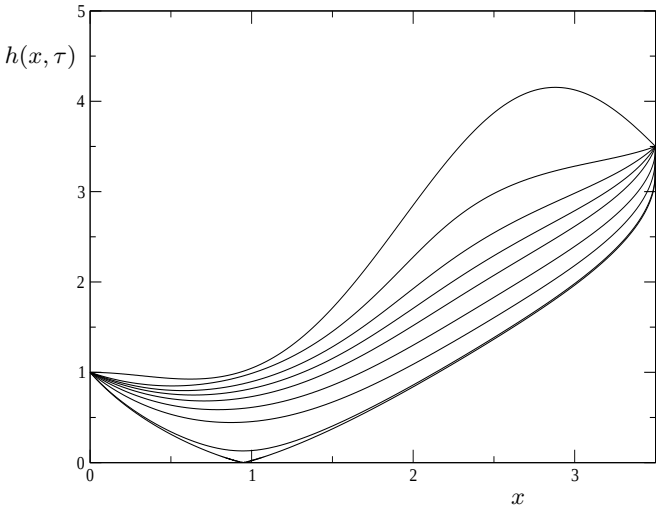

FIG. 5: A sequence of numerical profiles, obtained by simulating (4) in the liquid bridge geometry. The non-dimensional pressure has been set to $\Delta = -0.2$ for all simulations. The initial condition is given by (8), with a = 0.4.

Unfortunately, the geometry of an axisymmetric crystal dripping into a rectangular container is too complicated for us to replicate the boundary conditions exactly. Instead we use a simplified "liquid bridge" geometry where the crystal is held to a fixed radius at two ends, see Fig. 5. The left end corresponds to the nozzle opening, which has been normalized to one, the right end corresponds to the half-width $R_c = 3.5R_0$ of the container. The length of the computational domain is $L = R_c$. As initial condition we take a linear profile, modulated by a sine function of dimensionless amplitude a:

$$h_{init} = (1 + (R_c/R_0 - 1)x/L)\,(1 - a\sin(2\pi x/L)). \qquad (8)$$

The purpose of the amplitude a is to mimic the difference between the three experimental dripping events, without making an effort to approximate experimental initial conditions quantitatively. Among others, a fully quantitative description of the experiment would require us to keep the height dependence of the hydrostatic pressure, and to include the effects of the container walls.

The lower part of the profile sags somewhat under gravity, and pinch-off occurs near the upper part of the profile. In Fig. 6 we have re-plotted the square of the rescaled neck radius, using the same experimental data as before. Thus the asymptotic behavior (5) should give

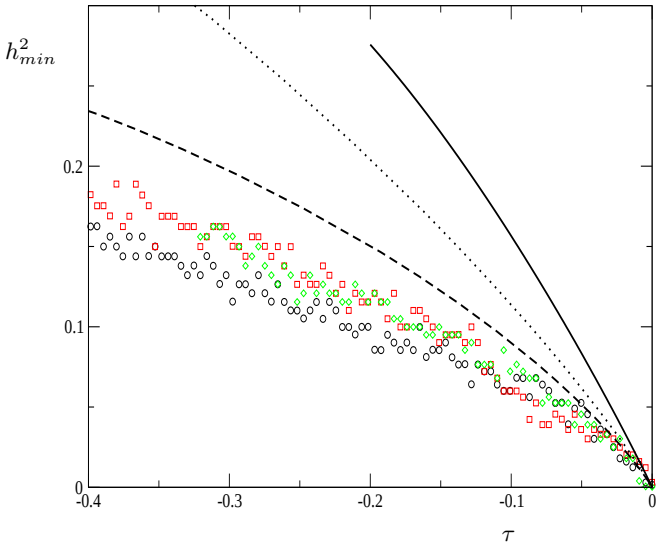

FIG. 6: The square of the rescaled neck radius, compared to both simulation and theory. Symbols are the same data as Fig. 4, the dashed and dotted lines are simulations of (4) with two different initial conditions, corresponding to $a = 0.7$ and 0.4, respectively. The full line is the asymptotic result (7).

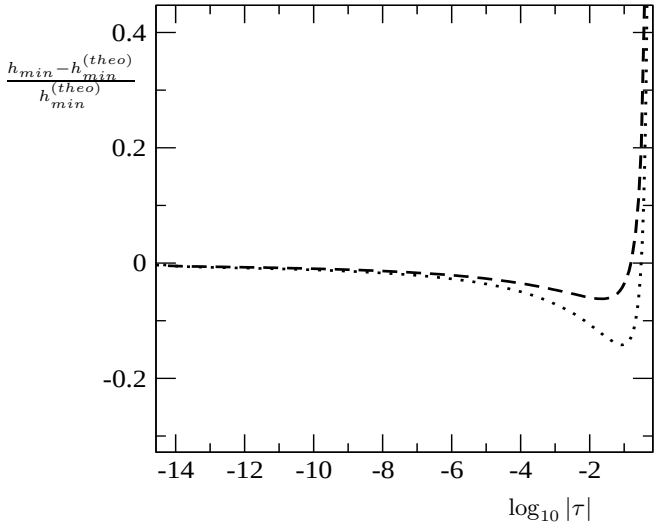

FIG. 7: Reduced deviations from the asymptotic result (9) for the two initial conditions, $a = 0.7$ (dashed) and 0.4 (dotted). Note the logarithmic scale on the abscissa.

a straight line of slope 2, which is included as the full line, including the logarithmic correction implied by (7). The result of two simulations for two different values of a is included as the dashed and the dotted line. The experiment is consistent with (7), if it is appreciated that asymptotics is only reached for $\tau < 0.02$.

This is also consistent with the direct numerical simulations of (4). Firstly, numerics starts to agree with asymptotics around the same reduced time that the experiment does. Secondly, the deviations from asymptotics are clearly non-universal: they depend strongly on the initial condition. Only as the asymptotic regime described by (7) is reached, does the system "forget" about the initial condition. This is illustrated in Fig. 7, where we have a plotted the deviation of the numerical solutions from the theoretical prediction (7):

$$h_{min} = \sqrt{2\tau}(1 - 1/(2l_\tau) + O(l_\tau^{-2})). \qquad (9)$$

Considerable differences between the two initial conditions persist to times $|\tau| \approx 10^{-4}$ away from the singularity, followed by very slow convergence toward (9). Eventually the deviations corresponding to the two numerical solutions become very close, suggesting that even higher order corrections to (9) are universal.

Thus although the experimental data seems to follow a 1/3-law in Fig.4, this appears to be fortuitous: by choosing an appropriate initial condition, solution of (4) can be constructed which closely resemble the experimental data. For other initial conditions, however, solutions remain far from the experimental data.

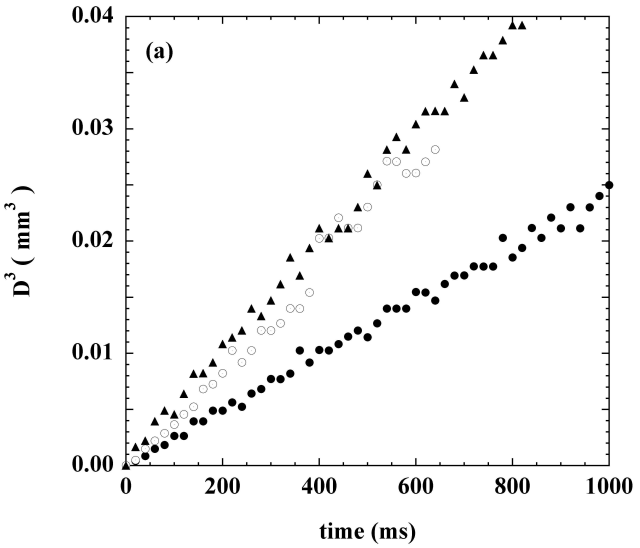

FIG. 8: As for dripping but now for their separation, the cube of the half gap D between the two crystals is proportional to the time Δt. Different symbols correspond to successive events recorded at T_{min} + 9 mK.

IV. RECOIL

We have also analyzed the retraction of the two tips of the crystal after it pinched off, and the results are shown in Fig. 8. Plotting the third power of the half gap D between the two tips, we find it being even more convincingly described by a 1/3 power law (but with varying amplitude).

However, once more do we believe that there is no par-

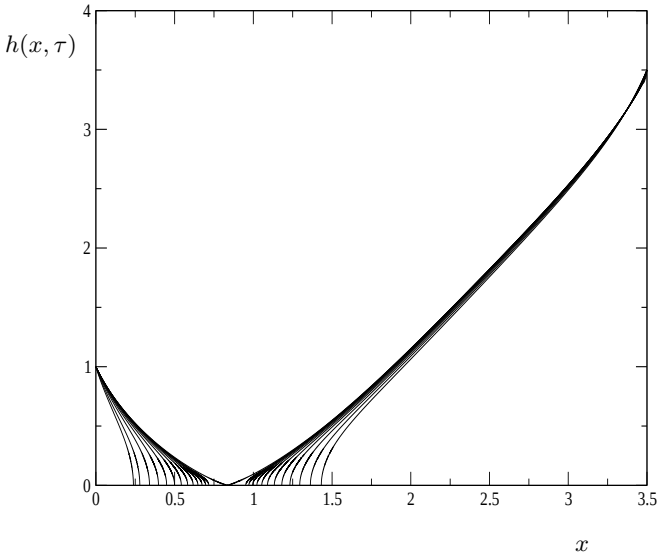

FIG. 9: A numerical simulation of (4) after pinch-off, corresponding to the profiles shown in Fig.5.

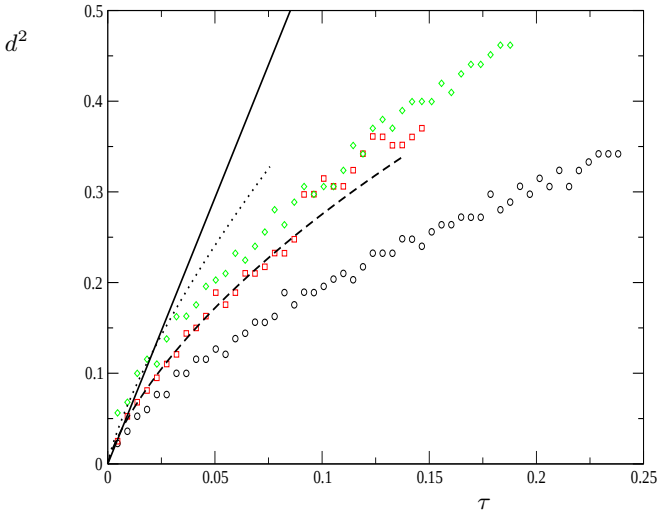

FIG. 10: The square of the rescaled half-gap, compared to to simulation and theory. Symbols are the same data as Fig. 4, the dashed and dotted lines are simulations of (4) with two different initial conditions, corresponding to $a = 0.7$ and 0.4, respectively. The full line corresponds to the retraction of a cone of opening angle 34.8 degrees.

ticular significance to this observation. To gain further insight, we compare to numerical simulations of (4), continuing the numerical simulations to times after pinch-off. When h_{min} has reached 10^{-3}, the neck is cut at the minimum and the tips on either side are spliced to a spherical cap. The results for the retracting tips, continuing the simulation shown in Fig. 5, is seen in Fig.9. Extracting the half-gap for the two initial conditions, one can compare the results to experiment, as shown in Fig.10. Again the results are very non-universal; however, the second simulation happens to give a result that closely matches two of the experimental data sets.

Again, the situation is very different from fluid drop breakup, where a universal solution for tip retraction was found [24]. The reason is the different character of the similarity description *before* breakup. Namely, in the fluid case the profile converges onto a universal shape for *all* values of the similarity variable ξ. This means that the behavior for large ξ can serve as a boundary condition for the solution after breakup, leading to a universal post-breakup solution. However, the validity of (7) is restricted to a small region $|\xi| \ll 1$, whereas everything outside of this region is non-universal. Hence the receding tip is in fact invading a region where the solution depends on the initial condition, and so also depends on initial conditions.

Nevertheless, one can estimate the retraction by approximating the profile at the moment of breakup by a cone of half angle θ, which is reasonable as seen in Fig.11. Let us begin by giving a rough argument for the speed of retraction, which captures the essential physics. Namely, we model the shape of each drop just after detachment as a cone with half angle θ which terminates as a spherical tip with radius R. The curvature is $\kappa = 2/R$ so that

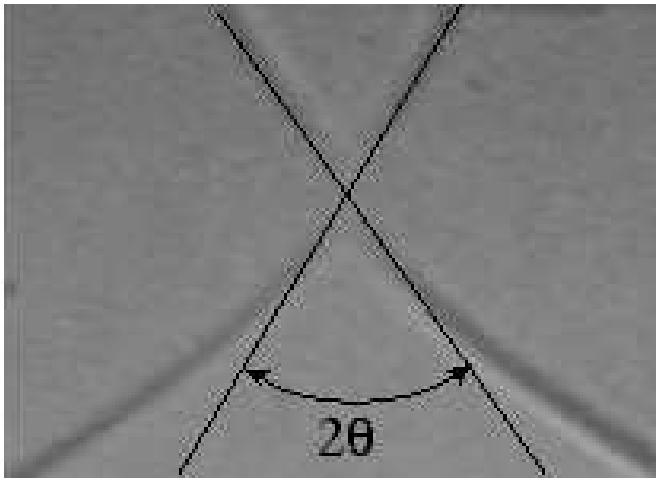

FIG. 11: After separation of the two crystalline drops, a gap opens. We approximate the shape of the two drops as cones with a spherical tip; here the half angle of the cone is 34.8 degrees.

$dR/d\tau = 2$ in non-dimensional variables. From simple geometry we find the dimensionless half gap $d = D/R_0$ between the two tips to be $d = R(1-\sin\theta)/\sin\theta$, so that the time dependence is

$$d^2 = 4\frac{(1-\sin\theta)^2}{\sin^2\theta}\tau. \qquad (10)$$

Of course, (10) cannot be completely quantitative, since the real shape of the receding tip will not have the

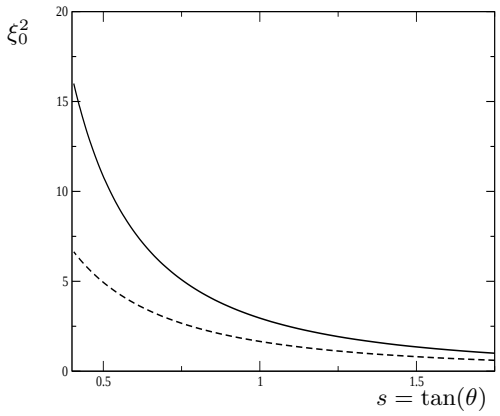

FIG. 12: The parameter ξ_0 characterizing the speed of retraction as function of the slope s of the cone. The full line is the result of our similarity theory, based on (12). The dashed line is the approximation (10).

precise form assumed above. A more accurate description can be obtained using the a similarity form analogous to (6):

$$h(x,t) = \tau^{1/2}\phi_a(\xi). \tag{11}$$

If the motion starts from a cone, for large arguments of ξ, ϕ_a must be a linear function with the same cone angle θ. Namely, far away from the moving tip, the time dependence on the right hand side of (11) drops out and one matches onto a static profile. Inserting (11) into (4) for $\Delta = 0$ one obtains the similarity equation

$$\frac{\phi_a''}{1+\phi_a'^2} + \xi\phi_a' - \phi_a - \frac{1}{\phi_a} = 0. \tag{12}$$

To obtain a solution of (12), we integrate (12) from a value $\xi = \xi_0$ to ∞. By the structure of (11), $d^2 = \xi_0^2\tau$; from an analysis near $\xi = \xi_0$ it follows that $\phi_a \approx 2((\xi-\xi_0)/\xi_0)^{1/2}$ near the tip. Using this local solution to construct an initial condition, there is a unique solution for each value of ξ_0. The asymptotic slope $s = \tan(\theta)$ for large ξ establishes a relationship between ξ_0 and the cone angle, shown in Fig. 12. Evidently, while (10) captures the right qualitative behavior, quantitative results require the solution of the full similarity equation (12).

For one set of data (red squares) we have fitted a cone to the profile (cf. Fig.11), and found an opening angle of about $\theta = 34.8$ degrees. From Fig.12, this corresponds to $\xi_0^2 = 5.87$, which is the slope of the full line in Fig. 10. The predicted asymptotic behavior, based on the simplifying assumption of initial cones, fits the data well, but again only at very small time after separation of the two drops.

In conclusion, we have studied the dripping of crystals where viscosity and inertia are negligible, and the dissipation is taking place only at the moving crystal surface. Asymptotically, pinch-off is described by mean-curvature flow, which exhibits an unusual type of self-similar behavior including logarithmic terms. The important physical consequence is that the approach to the singularity is extremely slow, so experimental observation, without the benefit of theory, may lead to an incorrect identification of scaling exponents. By the same token, a dependence on the initial condition persists to very close to pinch-off, as was recently observed for a related problem containing logarithms [25]. Thus statements about the universality of asymptotic behavior are virtually impossible to make by observation alone, in the absence of quantitative theoretical estimates of transients.

[1] J. Eggers, *Rev. Mod. Phys.* **69**, 865 (1997).
[2] J. Eggers, *Phys. Rev. Lett.* **71**, 3458 (1993).
[3] Y.J. Chen and P.H. Steen, J. Fluid Mech. **341**, 245-267 (1997).
[4] R. F. Day, E. J. Hinch, and J. R. Lister, Phys. Rev. Lett. **80**, 704 (1998).
[5] S. Balibar, H. Alles and A. Ya. Parshin, *Rev. Mod. Phys.* **77**, 317 (2005).
[6] R. Ishiguro, F. Graner, E. Rolley, and S. Balibar, *Phys. Rev. Lett.* **93**, 235301 (2004).
[7] F. Graner, R.M. Bowley, and P. Nozières, J. Low Temp. Phys. **80**, 113 (1990).
[8] H.J. Maris, Phys. Rev. **E 67**, 066309 (2003).
[9] P. Nozières, in: "Solids far from equilibrium", edited by C. Godrèche, Cambridge, (1992).
[10] E. Rolley, S. Balibar, F. Gallet, F. Graner, and C. Guthmann, Europhys. Lett. **8**, 523 (1989).
[11] G. Huisken, *J. Diff. Geom.* **31**, 285 (1990).
[12] S. B. Angenent and J. J. L. Velázquez, *J. reine angew. Math.* **482**, 15 (1997).
[13] E. Rolley, S. Balibar, and F. Gallet, Europhys. Lett. **2**, 247 (1986).
[14] R. Wagner, S.C. Steel, O.A. Andreeva, R. Jochemsen, and G. Frossati, Phys. Rev. Lett. **76**, 263 (1996).
[15] I.A. Todoshenko, H. Alles, H.J. Junes, A. Ya. Parshin, and V. Tsepelin, Physica **B 329-333**, 386 (2003).
[16] Y. Giga and R. V. Kohn, *Indiana Univ. Math. J.* **36**, 1 (1987).
[17] I. Cohen, M.P. Brenner, J. Eggers, and S.R. Nagel, *Phys. Rev. Lett.* **83**, 1147 (1999).
[18] A. Rothert, R. Richter, and I. Rehberg, *Phys. Rev. Lett.* **87**, 084501 (2001).
[19] A.U. Chen, P. K. Notz, and O. A. Basaran, *Phys. Rev. Lett.* **88**, 174501 (2002).
[20] J. Eggers and M.A. Fontelos, *to be published* (2006).
[21] H. Matano and F. Merle, *Comm. Pure Appl. Math.* **57**, 1494 (2004).
[22] J. Eggers, T. F. Dupont, *J. Fluid Mech.* **262**, 205 (1994).
[23] J. Eggers, *SIAM J. Appl. Math.* **60**, 1997 (2000).
[24] J. Eggers, *Phys. Fluids Phys. Fluids* **7**, 941 (1995).
[25] R. Bergmann et al., *Phys. Rev. Lett.* **96**, 154505 (2006).